Graphene spin diode: Strain-modulated spin rectification

Yunhua Wang, Yulan Liu, and B. Wang

Citation: Appl. Phys. Lett. **105**, 052409 (2014); doi: 10.1063/1.4892453
View online: https://doi.org/10.1063/1.4892453
View Table of Contents: http://aip.scitation.org/toc/apl/105/5
Published by the American Institute of Physics

APPLIED PHYSICS LETTERS **105**, 052409 (2014)

Graphene spin diode: Strain-modulated spin rectification

Yunhua Wang,[1] Yulan Liu,[2,a)] and B. Wang[1,a)]
[1]*Sino-French Institute of Nuclear Engineering and Technology, School of Physics and Engineering, State Key Laboratory of Optoelectronic Materials and Technologies, Sun Yat-sen University, Guangzhou 510275, China*
[2]*School of Engineering, Sun Yat-sen University, Guangzhou 510275, China*

(Received 29 April 2014; accepted 26 July 2014; published online 6 August 2014)

Strain effects on spin transport in a ferromagnetic/strained/normal graphene junction are explored theoretically. It is shown that the spin-resolved Fermi energy range can be controlled by the armchair direction strain because the strain-induced pseudomagnetic field suppresses the current. The spin rectification effect for the bias reversal occurs because of a combination of ferromagnetic exchange splitting and the broken spatial symmetry of the junction. In addition, the spin rectification performance can be tuned remarkably by manipulation of the strains. In view of this strain-modulated spin rectification effect, we propose that the graphene-based ferromagnetic/strained/normal junction can be used as a tunable spin diode. © *2014 AIP Publishing LLC*. [http://dx.doi.org/10.1063/1.4892453]

As a result of a weak intrinsic spin-orbit and hyperfine interactions,[1,2] the spin coherence length in graphene has been experimentally determined to be more than 1 μm at room temperature.[3] This ultra-long spin coherence length combined with the unique electronic structure means that graphene has attracted considerable attention from researchers in the fields of quantum transport and spin electronics applications. For practical implementation of graphene-based spintronics, two important problems, as demonstrated in semiconductor-based spintronics,[4,5] must be addressed. The first is how to inject and probe the spin in graphene, and the second is how to manipulate the spin transport in the graphene nanostructures and achieve practical application of these graphene nanostructures in spin electronic devices.

Three approaches have been presented to address the first problem, and are described as follows: (1) Spin is experimentally injected by ferromagnetic metal electrodes deposited on the graphene and separated by a tunneling barrier to enhance the injection efficiency, and spin is also detected by non-local spin valve measurements;[6–11] (2) Theoretical calculations predict that graphene nanoflakes can induce magnetic correlations as a result of their reduced dimensions and edge effects,[12,13] and a zigzag graphene ribbon that has been subjected to an in-plane electric field has complete spin polarization because of its half-metallic phase;[14,15] (3) Ferromagnetic graphene can be induced by a proximity effect between a ferromagnetic insulator and graphene,[16] and this proximity-effect-induced ferromagnetism has also been demonstrated experimentally.[17,18] Recent work on the second problem has addressed the spin transport in some typical graphene-based nanostructures, including the gate-induced quantum dot,[19] the ferromagnetic/barrier(ribbon)/ferromagnetic junction[20,21] and ferromagnetic barriers.[22] The gate-induced quantum dot may be applied in quantum computing, because of its advantageous spin qubits. The ferromagnetic/barrier (ribbon)/ferromagnetic junction, as a spin valve structure, may be used as a memory device, because of its large magnetoresistance effects. The ferromagnetic barriers may be designed as spin filters or spin splitters, because of their gate-controllable spin-resolved transport. However, there have been few studies of graphene spin diodes to date,[23] The spin diode, as an analogous version of the conventional charge diode, is an important spintronic component, where the spin polarization $p=(I_\uparrow+I_\downarrow)/(I_\uparrow-I_\downarrow)$ with respect to the bias (V_b) reversal, can be rectified (i.e., $p(-V_b)\neq p(V_b)$). A high-performance spin diode would require a remarkable spin rectification effect (i.e., $p(\pm V_b)\to 0$, whereas $p(\mp V_b)\approx C$, where C is a relative maximum value).

Recently, mechanical strain has been applied to modulate the electronic structures and transport in graphene nanostructures[24–33] by virtue of the anisotropic group velocity and the pseudomagnetic field that result from the strain-induced Dirac cone deformation and the K (K′) point displacements, respectively. Not only can reversible and controlled strains in graphene be realized using an atomic force microscope (AFM) tip[24] or suitable substrate patterning,[25–33] but the strain-induced changes in the electronic and optical properties of graphene can also be measured quantitatively by Raman spectroscopy.[26,27] As a result, mechanical strain has been shown to provide an important way to manipulate the electronic transport in graphene nanostructures. In this Letter, we report a strain-manipulated spin diode based on a ferromagnetic/strained/normal graphene junction, where the ferromagnetic exchange field and the broken spatial symmetry of the junction result in spin rectification, and the spin rectification performance can be tuned by adjusting the strain.

Hamiltonian, wave functions, and spin-dependent currents: We consider a ferromagnetic/strained/normal graphene junction, where a uniaxial strain is applied inside the middle region (S), and ferromagnetic and normal metal electrodes are deposited on the left (F) and right (N) regions, respectively, as shown in Fig. 1(a). The ferromagnetism in region F is induced by the proximity effect between the EuO

[a)]Authors to whom correspondence should be addressed. Electronic addresses: stslyl@mail.sysu.edu.cn and wangbiao@mail.sysu.edu.cn

electrode and the graphene, as demonstrated by recent experiments.[17,18] In the presence of a bias, V_b, a linear voltage drop with a dropping factor of $\beta = V_b/W$ will occur because of the uniform in-plane electric field between the left and right electrodes.[34] Because of the potential V_0 induced by the strain or by an additional gate in the middle region with width W, the potential barrier V_0 will lift the linear voltage drop completely, as shown in Fig. 1(b). In this graphene-based system, the excitation quasiparticles are described by the effective Hamiltonian as follows:

$$\begin{cases} \hat{H}_{F,\eta} = v_F(\vec{\sigma}_x p_x + \vec{\sigma}_y p_y) - \eta H_{ex}\vec{\sigma}_0, \\ \hat{H}_S = v_F U^{\dagger}(\theta)[\vec{\sigma}_x(1-\lambda_x\varepsilon)\hbar q_x + \vec{\sigma}_y(1-\lambda_y\varepsilon)\hbar q_y]U(\theta) + (V_0 - \beta x)\vec{\sigma}_0, \\ \hat{H}_N = v_F(\vec{\sigma}_x p_x + \vec{\sigma}_y p_y) - V_b\vec{\sigma}_0, \end{cases} \tag{1}$$

where $\vec{\sigma}_x$ and $\vec{\sigma}_y$ are the Pauli spin matrices, $v_F \approx 10^6\,\mathrm{m\cdot s^{-1}}$ is the Fermi velocity, η is $1(-1)$ for up (down) spin orientation, H_{ex} is the exchange field, and $\vec{\sigma}_0$ is the identity matrix. For the strain-dependent Hamiltonian,[32,33] θ is the angle between the strain direction and the graphene zigzag direction (labeled as the x-direction), $U(\theta) = \mathrm{diag}\,(1, e^{-i\theta})$ is the unitary matrix, and $\lambda_x = (|l/V_{pp\pi}||dV_{pp\pi}/dl|)|_{l=a_0} - 1 \approx 2.2$ is a factor that depends on the bond length l and the hopping integral function $V_{pp\pi}(l) = -2.7e^{-3.37(l/a_0-1)}$ between two neighboring carbon p orbitals;[28,32] $\lambda_y = -\mu\lambda_x \approx -0.308$ with Poisson's ratio $\mu = 0.14$, ε is the magnitude of the strain, and $\boldsymbol{q} = (q_x, q_y)^T$ measures the wave vector displacement $q_D = \pm[\kappa_0\varepsilon(1+\mu)\cos 3\theta/a_0, -\kappa_0\varepsilon(1+\mu)\sin 3\theta/a_0]$ (Refs. 32 and 33) from the shifted Dirac points, where $\kappa_0 \approx 1.6$ and $a_0 = 0.142\,\mathrm{nm}$ is the C-C distance. The energy gap is not considered here because the magnitude of the strain applied in this work is limited to within 20%, where the gap cannot be opened up.[31] It is convenient to simplify the notations of all quantities by introducing dimensionless units with a basic length scale $L_0 = 81.8\,\mathrm{nm}$ and a corresponding energy scale $E_0 = \hbar v_F/L_0 \approx 8.113\,\mathrm{meV}$. Taking the conservation of k_y into account and using Eq. (1), we can write the wave functions of these particles that are moving along the $\pm x$ directions in all regions as $\boldsymbol{\psi}^{\pm}(x,y) = \boldsymbol{\psi}^{\pm}(x)e^{ik_y y}$, where $\boldsymbol{\psi}^{\pm}{}_{F,\eta}(x)$ and $\boldsymbol{\psi}^{\pm}{}_N(x)$ satisfy

$$\begin{cases} \boldsymbol{\psi}^{\pm}{}_{F,\eta}(x) = e^{\pm ik_\eta x}(1, \pm g_\eta e^{\pm i\gamma_\eta})^T, \\ \boldsymbol{\psi}^{\pm}{}_N(x) = e^{\pm ik_x x}(1, \pm\chi e^{\pm i\varphi})^T, \end{cases} \tag{2}$$

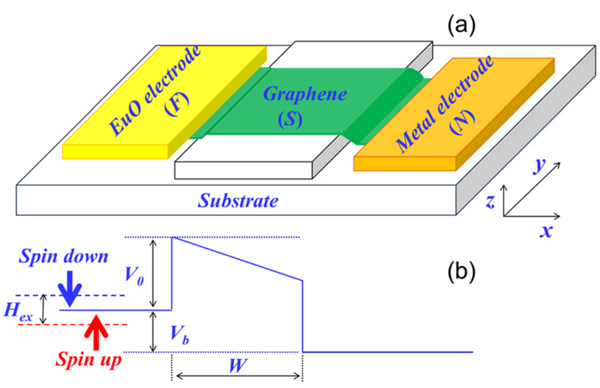

FIG. 1. (a) Spin diode model of the ferromagnetic/strained/normal graphene junction and (b) the corresponding conduction-band edge profiles, where H_{ex} is the exchange field, V_0 is the potential, V_b is the bias, and W is the width of the strained region.

where $\gamma_\eta = \sin^{-1}(k_y/|E+\eta H_{ex}|)$, $k_\eta = |E+\eta H_{ex}|\cos\gamma_\eta$, $g_\eta = \mathrm{sgn}(E+\eta H_{ex})$, $\varphi = \sin^{-1}(k_y/|E+V_b|)$, $k_x = |E+V_b|\cos\varphi$, and $\chi = \mathrm{sgn}(E+V_b)$. Because of the linear voltage drop, the boundary of the potential barriers and the smoothness of the strain, the wave functions in the entire middle region are no longer plane waves. It is convenient to separate this middle region into a series of reasonably narrow layers with a uniform width of $a = W/N \gg a_0$, where N is the number of narrow layers. A reasonable width ensures that the wave functions inside each narrow layer can be viewed approximately as a plane wave

$$\boldsymbol{\psi}^{\pm}{}_{S,j}(x) = e^{\pm ik_{x,j}x}(1, \pm s_j e^{\pm i\varphi_j})^T, \tag{3}$$

with different longitudinal wave vectors of $k_{x,j} = (1-\lambda_x\varepsilon)^{-1}|E+V_0-\beta x_j|\cos\varphi_j$ in the jth narrow layer ($j = 1, 2, \ldots, N$), where $\varphi_j = \sin^{-1}[(k_y - q_{Dy})/|E+V_0-\beta x_j|]$ and $s_j = \mathrm{sgn}(E+V_0-\beta x_j)$. By assuming that the incident quasiparticles have normalized probability densities, we can write the total wave functions in the corresponding regions as

$$\begin{cases} \boldsymbol{\psi}_{F,\eta}(x) = \boldsymbol{\psi}^{+}_{F,\eta}(x)/\sqrt{2} + r_\eta\boldsymbol{\psi}^{-}_{F,\eta}(x)/\sqrt{2}, \\ \boldsymbol{\psi}_{S,j}(x) = a_j\boldsymbol{\psi}^{+}_{S,j}(x)/\sqrt{2} + b_j\boldsymbol{\psi}^{-}_{S,j}(x)/\sqrt{2}, \\ \boldsymbol{\psi}_N(x) = t_\eta\sqrt{k_\eta(E+V_b)/k_x(E+\eta H_{ex})}\,\boldsymbol{\psi}^{+}_N(x)/\sqrt{2}, \end{cases} \tag{4}$$

where r_η and t_η are the reflection and transmission coefficients, respectively, and a_j and b_j are unknown complex coefficients that both contain a factor of the strain-changed group velocity.[33,35] The factor $\sqrt{k_\eta(E+V_b)/k_x(E+\eta H_{ex})}$ guarantees probability current normalization and the spin-flip is assumed to be quite weak because of the ultra-long spin coherence length.[16,19–23] To guarantee the requirements of the continuity equation, these wave functions must be continuous at any boundary. Therefore, based on the continuity of $\boldsymbol{\psi}(x)$, we can obtain the reflection and transmission coefficients. By taking all possible particle trajectories into account, we can write the spin-dependent current as

$$\begin{aligned} I_\eta/I_0 = &\int_{-\infty}^{+\infty}\int_{-\pi/2}^{+\pi/2} |t_\eta(E,\gamma_\eta,V_b,\varepsilon)|^2|E+\eta H_{ex}| \\ &\times[f(E-E_F) - f(E-E_F+V_b)]\cos\gamma_\eta dE d\gamma_\eta, \end{aligned} \tag{5}$$

where $f(x) = 1/(e^{x/k_BT}+1)$ is the Fermi-Dirac distribution function, and $I_0 = 2ev_F L_y/(2\pi\hbar v_F)^2$ is the current unit with

y-direction width L_y and a factor of 2 because of the valley degeneracy. The spin polarization is defined by $p = (I_\uparrow + I_\downarrow)/(I_\uparrow - I_\downarrow)$.

Strain effects on the spin-resolved Fermi energy range: Figure 2 shows the spin-dependent current as a function of the Fermi energy E_F. To ensure that the electron density of states agrees well with that of a real system, some valid parameter values were used: $W = 1$, $V_0 = 6$, $N = 20$, $V_b = 10/E_0$, $k_BT = 0.5/E_0$, and $H_{ex} = 5/E_0$, where $H_{ex} = 5/E_0$ and $k_BT = 0.5/E_0$ reflect the typical exchange splitting field and the temperature of liquid helium, respectively. First, we investigate the spin-resolved Fermi energy range, where the spin-splitting currents occur without applied strain (i.e., $\varepsilon = 0\%$). From Figs. 2(a) and 2(b), we can clearly see that the spin-up current nearly agrees with the spin-down current when $E_F > V_0$, and the spin-up current is obviously different to the spin-down current when $E_F \leq V_0$. This means that the spin-resolved currents occur only when $E_F \leq V_0$ if strain is never applied to the structure. Physically, classical tunneling for $E_F > V_0$ leads to nearly the same transmission for the spin-up and spin-down electrons, while Klein tunneling for $E_F \leq V_0$ leads to remarkably spin-resolved transmissions for both spin-up and spin-down electrons.[36] This combination of classical tunneling and Klein tunneling therefore ultimately restricts the spin-resolved Fermi energy range to $E_F \leq V_0$.

We also investigate the strain effects on the spin-resolved Fermi energy range. In this work, we consider double typical direction strains including the zigzag ($\theta = 0$) and armchair ($\theta = \pi/2$) directions. For comparison with the spin-dependent currents without applied strain, we use the identical values for W, V_0, V_b, k_BT, and H_{ex}. Figure 2(a) shows that the zigzag direction strain can tune the spin-splitting currents but that it has no effect on the spin-resolved Fermi energy range. However, with increased armchair direction strain, the previous spin-resolved Fermi energy range of $E_F \leq V_0$ is obviously suppressed, and even becoming a current gap, and then finally moves towards $E_F > V_0$, as shown in Fig. 2(b). Physically, one remarkable difference between the effects of the zigzag and armchair direction strains is that they have completely different Dirac point displacements, which can introduce pseudomagnetic fields that suppress the current.[28–33] The Dirac point under the zigzag direction strain never shifts with $q_{Dy} = 0$, while the Dirac point displacement increases dramatically under enhanced armchair direction strain, with $-q_{Dy} \approx 84.55\varepsilon$. Therefore, the change in the spin-resolved Fermi energy range under armchair strain is a result of the strain-induced Dirac point shift. This means that we can adjust the armchair direction strain to control the spin-resolved Fermi energy range.

Spin-dependent I-V curves and strain effects on the spin polarization: Next, we investigate the spin-dependent *I-V* curves (i.e., the current-bias curves), which can decide whether the ferromagnetic/strained/normal graphene junction presented here has spin rectification (diode) effects (i.e., $p(-V_b) \neq p(V_b)$). If we consider that the spin-resolved Fermi energy range for the zigzag direction strain is within $E_F \leq V_0$, while that for the armchair direction strain moves towards $E_F > V_0$, we can then take the Fermi energies to be $E_F = 2.5$ and $E_F = 9.5$ for the zigzag and armchair strains, respectively. The structural parameters are identical to those used in Fig. 2. The spin-dependent current-bias curves obtained using these values are plotted in Fig. 3. It is clearly shown that, in the presence of a positive bias, the spin-resolved currents always occur, while under negative bias, the spin-splitting of the currents is very weak. This demonstrates that the ferromagnetic/strained/normal graphene junction has an obvious spin rectification (diode) effect. The spin rectification effect is a result of the spatial structural asymmetry induced by the left ferromagnetic electrode and the right metal electrode. In other words, the broken spatial symmetry combined with the lifted spin degeneracy from the ferromagnetic exchange field results in a spin rectification effect with respect to the bias reversal. In addition, in Fig. 3, we can see that both of the zigzag and armchair direction strains provide obvious tunability of the spin-splitting currents. Usually, for a spin diode structure, such as the ferromagnetism/quantum-dot/metal structure,[37] the diluted magnetic semiconductor heterostructure,[38] the ferromagnetic/molecular wire/metal structure,[39] and the asymmetrical spin-orbit coupling electron waveguide structure,[40] either a gate-controlled voltage or a magnetic field is applied to tune the spin rectification effect. This Letter shows that the mechanical strain can also be used to manipulate the spin rectification effect in a spin diode based on the ferromagnetic/strained/normal graphene junction.

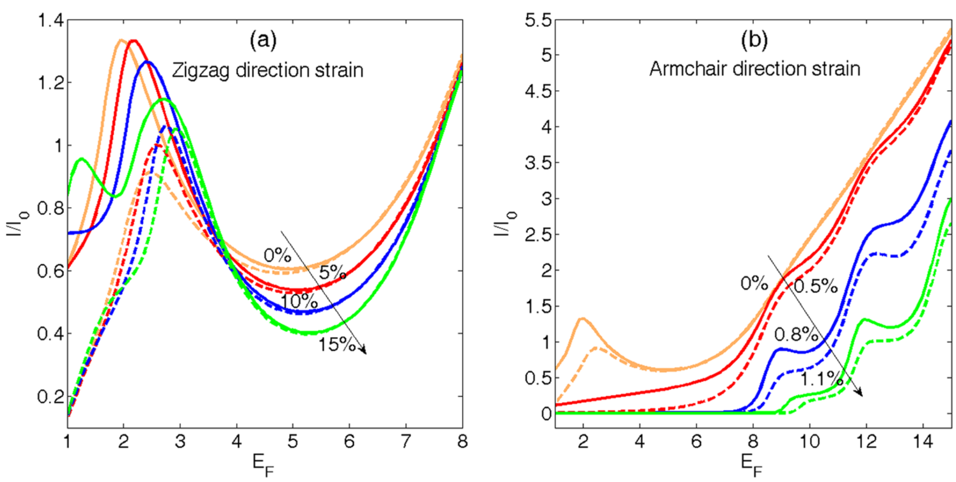

FIG. 2. Spin-up (solid line) and spin-down (dashed line) currents as a function of the Fermi energy E_F, for $W = 1$, $V_0 = 6$, $N = 20$, $V_b = 10/E_0$, $k_BT = 0.5/E_0$, and $H_{ex} = 5/E_0$. (a) The effects of zigzag direction strain for $\varepsilon = 0\%$, 5%, 10%, and 15% along the direction of the arrow. (b) The effects of the armchair direction strain for $\varepsilon = 0\%$, 0.5%, 0.8%, and 1.1% along the direction of the arrow.

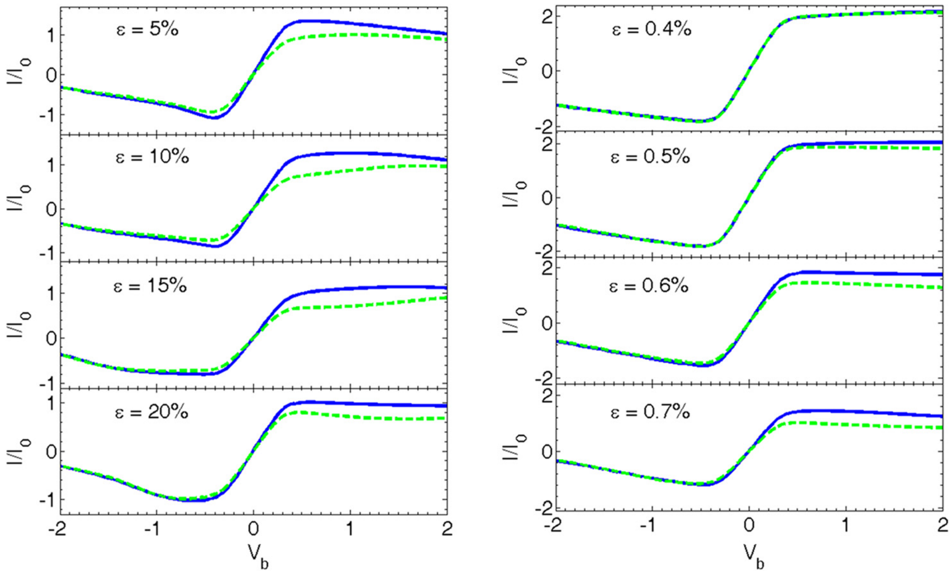

FIG. 3. Spin-up (solid line) and spin-down (dashed line) current-bias (I-V) curves for $W=1$, $V_0=6$, $N=20$, $k_BT=0.5/E_0$, and $H_{ex}=5/E_0$. Left panel: effects of the zigzag direction strain with $E_F=2.5$; Right panel: effects of the armchair direction strain with $E_F=9.5$.

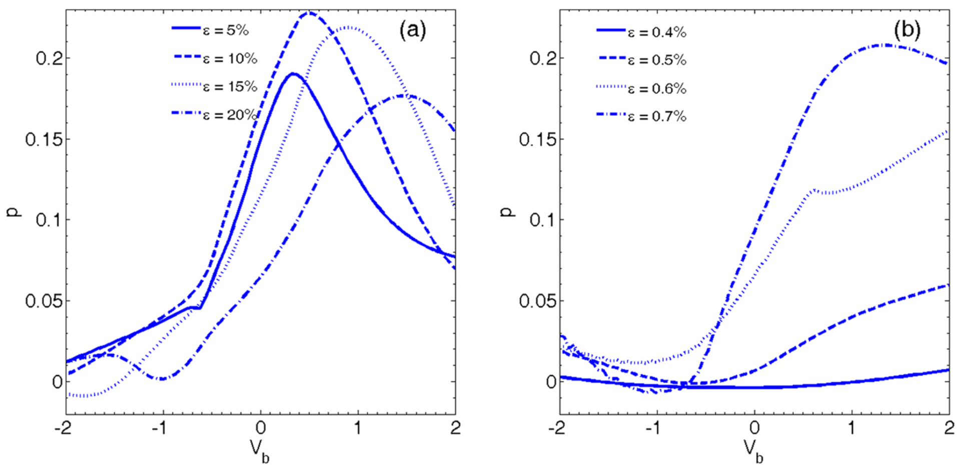

FIG. 4. Spin polarization as a function of the bias V_b for the same parameters that were used in Fig. 3. (a) Effects of the zigzag direction strain with $E_F=2.5$. (b) Effects of the armchair direction strain with $E_F=9.5$.

In Fig. 4, to demonstrate the strain effects on the spin polarization in the graphene spin diode, we present the spin polarization as a function of the bias under different strain magnitudes. In the figure, we can clearly see that the spin polarizations show typical asymmetry for the contrary bias, i.e., $p(-V_b) \neq p(V_b)$. In Fig. 4(a), with increasing zigzag direction strain, the asymmetrical bias peaks move towards the higher voltage range. This means that we can adjust the zigzag direction strain to control the spin rectification bias range. In Fig. 4(b), with increasing armchair direction strain, the spin rectifications are dramatically enhanced. It is also possible to reduce the spin rectifications under the armchair direction strain (although it is not shown in this Letter). Therefore, we must carefully manipulate the armchair direction strain to strengthen the spin rectifications. Finally, in real situations, some of the boundary effects of the potential barriers and the smoothness of the strain always have obvious effects on the spin-resolved currents, while we can also find that the strain-modulated spin rectifications are maintained by adopting a typical potential profile and a strain profile.[33]

In summary, we have explored the effects of strain on the spin-resolved currents and spin polarizations in a ferromagnetic/strained/normal graphene junction as a function of the Fermi energy and the bias voltage. We found that the spin-resolved Fermi energy range can be changed by the armchair direction strain through the strain-induced Dirac point displacement. The spin rectification effect with respect to the bias reversal occurs because of the broken spatial symmetry induced by the ferromagnetic and metallic electrodes used in this junction. In addition, it is shown that the spin rectification effect can be adjusted remarkably by manipulating the zigzag and armchair direction strains. On the basis of this strain-modulated spin rectification effect, we propose the use of the ferromagnetic/strained/normal graphene junction as a tunable spin diode.

We are grateful for the support from the National Natural Science Foundation through the funds (Grant Nos. 11232015 and 11072271), and the Research Fund for the Doctoral Program of Higher Education of China (Grant No. 20120171110005).

[1]C. L. Kane and E. J. Mele, Phys. Rev. Lett. **95**, 226801 (2005).
[2]D. Huertas-Hernando, F. Guinea, and A. Brataas, Phys. Rev. B **74**, 155426 (2006).
[3]N. Tombros, C. Józsa, M. Popinciuc, H. T. Jonkman, and B. J. van Wees, Nature **448**, 571 (2007).
[4]S. A. Wolf, D. D. Awschalom, R. A. Buhrman, J. M. Daughton, S. von Molnár, M. L. Roukes, A. Y. Chtchelkanova, and D. M. Treger, Science **294**, 1488 (2001).

[5] I. Zutic, J. Fabian, and S. D. Sarma, Rev. Mod. Phys. **76**, 323 (2004).
[6] E. W. Hill, A. K. Geim, K. Novoselov, F. Schedin, and P. Blake, IEEE Trans. Magn. **42**, 2694 (2006).
[7] M. Ohishi, M. Shiraishi, R. Nouchi, T. Nozaki, T. Shinjo, and Y. Suzuki, Jpn. J. Appl. Phys., Part 2 **46**, L605 (2007).
[8] C. Józsa, M. Popinciuc, N. Tombros, H. T. Jonkman, and B. J. van Wees, Phys. Rev. Lett. **100**, 236603 (2008).
[9] S. Cho, Y. F. Chen, and M. S. Fuhrer, Appl. Phys. Lett. **91**, 123105 (2007).
[10] W. Han, K. Pi, W. Bao, K. M. McCreary, Y. Li, W. H. Wang, C. N. Lau, and R. K. Kawakami, Appl. Phys. Lett. **94**, 222109 (2009).
[11] W. Han, W. H. Wang, K. Pi, K. M. McCreary, W. Bao, Y. Li, F. Miao, C. N. Lau, and R. K. Kawakami, Phys. Rev. Lett. **102**, 137205 (2009).
[12] O. V. Yazyev, Rep. Prog. Phys. **73**, 056501 (2010).
[13] W. L. Wang, S. Meng, and E. Kaxiras, Nano Lett. **8**, 241 (2008).
[14] Y.-W. Son, M. Cohen, and S. G. Louie, Nature **444**, 347 (2006).
[15] E.-J. Kan, Z. Li, J. Yang, and J. G. Hou, Appl. Phys. Lett. **91**, 243116 (2007).
[16] H. Haugen, D. Huertas-Hernando, and A. Brataas, Phys. Rev. B **77**, 115406 (2008).
[17] A. G. Swartz, P. M. Odenthal, Y. Hao, R. S. Ruoff, and R. K. Kawakami, ACS Nano **6**, 10063 (2012).
[18] J. Klinkhammer, D. F. Förster, S. Schumacher, H. P. Oepen, T. Michely, and C. Busse, Appl. Phys. Lett. **103**, 131601 (2013).
[19] B. Trauzettel, D. V. Bulaev, D. Loss, and G. Burkard, Nat. Phys. **3**, 192 (2007).
[20] W. Y. Kim and K. S. Kim, Nat. Nanotechnol. **3**, 408 (2008); Y. T. Zhang, H. Jiang, Q. F. Sun, and X. C. Xie, Phys. Rev. B **81**, 165404 (2010); B. Zhou, X. Chen, H. Wang, K. Ding, and G. Zhou, J. Phys.: Condens. Matter **22**, 445302 (2010); J. C. Chen, S. G. Cheng, S. Q. Shen, and Q. F. Sun, J. Phys.: Condens. Matter **22**, 035301 (2010).
[21] C. Bai and X. Zhang, Phys. Lett. A **372**, 725 (2008); J. Zou, G. Jin, and Y. Ma, J. Phys.: Condens. Matter **21**, 126001 (2009); V. H. Nguyen, A. Bournel, and P. Dollfus, J. Appl. Phys. **109**, 073717 (2011).
[22] T. Yokoyama, Phys. Rev. B **77**, 073413 (2008); Y. X. Li, Eur. Phys. J. B **68**, 119 (2009); F. Zhai and L. Yang, Appl. Phys. Lett. **98**, 062101 (2011); Y. Wang, Y. Liu, and B. Wang, Physica B **437**, 71 (2014).
[23] Graphene spin diode is scarce, while graphene ribbon spin diode has been studied in two current works, M. Zeng, L. Shen, M. Zhou, C. Zhang, and Y. Feng, Phys. Rev. B **83**, 115427 (2011); X. Zhai and G. Jin, Solid State Commun. **152**, 2109 (2012).
[24] C. Lee, X. Wei, J. W. Kysar, and J. Hone, Science **321**, 385 (2008).
[25] K. S. Kim, Y. Zhao, H. Jang, S. Y. Lee, J. M. Kim, K. S. Kim, J. H. Ahn, P. Kim, J. Choi, and B. H. Hong, Nature **457**, 706 (2009).
[26] Z. H. Ni, T. Yu, Y. H. Lu, Y. Y. Wang, Y. P. Feng, and Z. X. Shen, ACS Nano **2**, 2301 (2008).
[27] T. M. G. Mohiuddin, A. Lombardo, R. R. Nair, A. Bonetti, G. Savini, R. Jalil, N. Bonini, D. M. Basko, C. Galiotis, N. Marzari, K. S. Novoselov, A. K. Geim, and A. C. Ferrari, Phys. Rev. B **79**, 205433 (2009).
[28] V. M. Pereira, A. H. Castro Neto, and N. M. R. Peres, Phys. Rev. B **80**, 045401 (2009).
[29] V. M. Pereira and A. H. Castro Neto, Phys. Rev. Lett. **103**, 046801 (2009).
[30] F. Guinea, M. I. Katsnelson, and A. K. Geim, Nat. Phys. **6**, 30 (2010).
[31] S. M. Choi, S. H. Jhi, and Y. W. Son, Phys. Rev. B **81**, 081407(R) (2010).
[32] F. M. D. Pellegrino, G. G. N. Angilella, and R. Pucci, Phys. Rev. B **84**, 195404 (2011); **85**, 195409 (2012).
[33] Y. Wang, Y. Liu, and B. Wang, Appl. Phys. Lett. **103**, 182603 (2013); Appl. Phys. Express **6**, 065102 (2013).
[34] Y. Song, H. C. Wu, and Y. Guo, Appl. Phys. Lett. **102**, 093118 (2013); K. S. Novoselov, A. K. Geim, S. V. Morozov, D. Jiang, Y. Zhang, S. V. Dubonos, I. V. Grigorieva, and A. A. Firsov, Science **306**, 666 (2004).
[35] Y. Wang, Y. Liu, and B. Wang, Physica E **48**, 191 (2013); **53**, 186 (2013).
[36] One can similarly obtain the spin-dependent Klein tunneling from this work, M. I. Katsnelson, K. S. Novoselov, and A. K. Geim, Nat. Phys. **2**, 620 (2006).
[37] F. M. Souza, J. C. Egues, and A. P. Jauho, Phys. Rev. B **75**, 165303 (2007); I. Weymann and J. Barnaś, Appl. Phys. Lett. **92**, 103127 (2008); C. A. Merchant and N. Marković, J. Appl. Phys. **105**, 07C711 (2009).
[38] Y. Guo, X. Y. Chen, F. Zhai, B. L. Gu, and Y. Kawazoe, Appl. Phys. Lett. **80**, 4591 (2002); F. Zhai, Y. Guo, and B. L. Gu, J. Appl. Phys. **94**, 5432 (2003).
[39] H. Dalgleish and G. Kirczenow, Phys. Rev. B **73**, 235436 (2006); R. Q. Wang and L. B. Hu, Phys. Lett. A **374**, 4156 (2010).
[40] F. Zhai, K. Chang, and H. Q. Xu, Appl. Phys. Lett. **92**, 102111 (2008).